

Curve Crossing for Low-Energy Elastic Scattering of He^+ by Ne^\dagger

S. M. Bobbio,* L. D. Doverspike, and R. L. Champion

Department of Physics, College of William and Mary, Williamsburg, Virginia 23185

(Received 10 April 1972; revised manuscript received 15 September 1972)

The perturbation seen in the experimental differential elastic-scattering cross section for the 40-eV $\text{He}^+ + \text{Ne}$ system has been attributed to a single crossing of two intermolecular potential-energy curves. A new theoretical treatment of the curve-crossing problem, namely, that of Delos and Thorson, is employed to obtain the crossing probabilities and phases associated with the crossing. These are determined by utilizing *ab initio* potentials involved in the crossing and are further used in a partial-wave calculation of the cross section, which is compared with our experiment. The origin of the oscillatory structure observed in the differential cross section is discussed in semiclassical terms by defining the problem in terms of two pseudo-deflection-functions. A rainbow effect is shown to be related to a particular feature (a maximum rather than a minimum) of these deflection functions.

I. INTRODUCTION

Extensive studies of the differential scattering of singly charged rare-gas ions by rare-gas atoms have been reported by several laboratories.¹ These efforts have contributed greatly to our theoretical understanding of elastic scattering and various inelastic processes which generally involve several potentials and interactions of the electronic states of the collision partners. The more detailed theoretical analysis which is needed to cope with such problems is currently in a state of rapid development. For example, a unified formal treatment of the two-state potential-curve-crossing problem for atomic collisions has just been completed by Delos and Thorson²; this treatment of the two-state problem being more complete than the standard Landau-Zener-Stuckelberg method which has been used in many calculations heretofore. Briefly, the approach developed by Delos and Thorson essentially reduces the problem of solving the two coupled second-order wave equations to the easier task of solving three first-order "trajectory equations." Their solutions are readily connected with the S-matrix elements describing the scattering amplitudes for the two-state system. The inputs to such a calculation are the potential-energy curves in question (either a diabatic or adiabatic representation will suffice) and the interaction term $V_{12}(R)$ in the vicinity of the crossing.

The purposes of this paper are to (i) demonstrate the results of such a calculation for the scattering system $\text{He}^+ + \text{Ne}$ ($E_{\text{c.m.}} = 40$ eV), where the initial inputs are from an *ab initio* calculation of Sidis and Lefebvre-Brion³ for the NeHe^+ molecular ion; (ii) compare these results with the differential elastic-scattering cross section measured in this laboratory; (iii) suggest a slight modification in the potentials (which probably is not unique) which

is necessary to bring certain features of the calculation and experiment into fairly good agreement; (iv) discuss the origin of the observed scattering features in semiclassical terms.

It should be pointed out that, although the Sidis-Lefebvre-Brion calculations show two relatively closely spaced crossings (BC at $1.86a_0$ and BC' at $1.77a_0$), it is our intention to discuss the experimental observation in terms of two states only, namely, $B^2\Sigma^+$ and $C^2\Sigma^+$. This assumption is plausible in that (a) the classically predicted c.m. scattering angles corresponding to the two crossings are well separated (52.2° and 64.1° , respectively); and (b) the semiclassical mechanical calculation based on two states will be seen to show all the qualitative features experimentally resolved. Conversely, the experimental observation does not show two sets of pronounced oscillations spaced by 12° , as one might expect if both the BC and BC' crossings had equal effect. Furthermore, the two-state assumption is necessitated since, to our knowledge, a viable three-state theory does not exist at present.

II. SUMMARY OF THEORY

The recent theoretical work of Delos and Thorson² (to which the reader should refer for complete details of the theory) has reduced the two coupled Schrödinger equations which are assumed to govern the dynamics of the scattering to the three first-order equations:

$$\begin{aligned} \frac{dZ}{dt}(l, t) &= -\frac{[1 - Z^2(l, t)]^{1/2}}{2(1 + t^2)} \cos[\Delta + \Gamma_2(l, t) - \Gamma_1(l, t)], \\ \frac{d\Gamma_1}{dt}(l, t) &= \frac{Z(l, t)}{2(1 + t^2)[1 - Z^2(l, t)]^{1/2}} \\ &\quad \times \sin[\Delta + \Gamma_2(l, t) - \Gamma_1(l, t)], \\ \frac{d\Gamma_2}{dt}(l, t) &= \frac{[1 - Z^2(l, t)]^{1/2}}{2(1 + t^2)Z(l, t)} \sin[\Delta + \Gamma_2(l, t) - \Gamma_1(l, t)], \end{aligned} \quad (1)$$

with

$$\Delta = -\frac{\beta}{2} \int_{-\epsilon}^t \frac{(1+\tau^2)^{1/2}}{(\epsilon+\tau)^{1/2}} d\tau$$

and the boundary conditions

$$Z(l, -\epsilon) = 0, \quad \Gamma_1(l, -\epsilon) = 0, \quad \Gamma_2(l, -\epsilon) = -\pi.$$

The quantities β and ϵ depend upon the angular-momentum quantum number l and the potential parameters through the relations

$$\epsilon = \frac{1}{2} \left(E - V_1(R_c) - \frac{\hbar^2(l + \frac{1}{2})^2}{2\mu R_c^2} \right) \times \left(\frac{dV_1}{dR} \Big|_{R_c} - \frac{dV_2}{dR} \Big|_{R_c} \right) / V_{12} F(R_c),$$

$$\beta = \frac{4}{\hbar} \left[(\mu V_{12}^3(R_c)) / \left(\frac{dV_1}{dR} \Big|_{R_c} - \frac{dV_2}{dR} \Big|_{R_c} \right) F(R_c) \right]^{1/2},$$

where $V_{12}(R_c)$ is the interaction term, V_1 and V_2 are the two potential curves as defined in Fig. 1, $F(R_c)$ is the geometric average of $(dV_{1\text{eff}}/dR)_{R_c}$ and $(dV_{2\text{eff}}/dR)_{R_c}$, and the subscript c refers to the crossing.

The set of Eqs. (1) are numerically integrated for each value of l from $t = -\epsilon$ to $t = +\infty$ [in practice the quantities $\Gamma_1(l, t)$, $\Gamma_2(l, t)$, and $Z(l, t)$ have attained their asymptotic values for $t = +30$, at which point the integration is halted]. The solutions $\Gamma_1(l)$, $\Gamma_2(l)$, and $Z(l)$ have the same general validity in the semiquantal mechanical regime as do the JWKB phase shifts, even in the important case where the classical turning point is

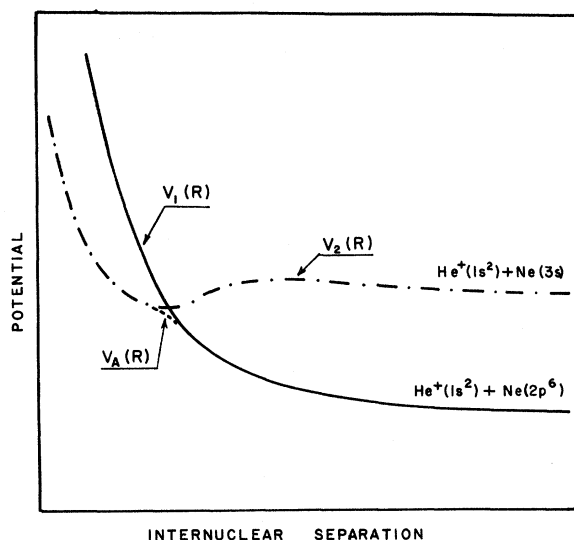


FIG. 1. Schematic diagram of the potential curves for Ne-He⁺ discussed in this paper. $V_1(R)$ and $V_2(R)$ are the results of diabatic calculations and $V_A(R)$ is an assumed adiabatic interaction.

close to the crossing. Moreover, these solutions are connected with the elastic-scattering problem in the following way:

$$f(\theta) = \frac{1}{2ik} \sum_{l=0}^{\infty} (2l+1) P_l(\cos\theta) [S(l) - 1],$$

$$S(l) = Z^2(l) \exp\{2i[\eta_a(l) - \Gamma_2(l)]\} + [1 - Z^2(l)] \exp\{2i[\eta_a(l) + \Gamma_1(l)]\}.$$

Here $\eta_a(l)$ is the JWKB phase shift resulting from scattering by the ground-state adiabatic potential [i. e., $V_a(R)$ in Fig. 1].

For a small interaction term $V_{12}(R_c)$, it is necessary to solve the set (1) only over a relatively narrow range of l around l_c . Outside this range the Landau-Zener transition probability is a very good approximation to $Z^2(l)$; $\Gamma_1(l)$ is constant, approximately $\frac{1}{4}\pi$; and $\Gamma_2(l) + \pi$ is essentially the difference between $\eta_a(l)$ and $\eta_d(l)$, where the latter quantity is the phase shift corresponding to the diabatic potential [i. e., $V_1(R)$ in Fig. 1] which connects to the ground state of the separated atom and ion.

III. ANALYSIS OF SCATTERING DATA

In Fig. 2 are shown the experimental elastic-scattering differential cross sections for the He⁺+Ne system at three different energies. At 6 eV the elastic-scattering differential cross section is a smooth monotonically decreasing function since the collision energy is not sufficient to sample the crossing. Thus, at this low energy, the cross section is entirely determined by the potential $V_1(R)$ in Fig. 3. At 30 eV a perturbation in the differential cross section appears at large angles. At 40 eV the major portion of this perturbation is centered in the angular range of our apparatus described in Ref. 4, and it is to these data that the present analysis will be directed. It will be assumed in the subsequent analysis that these perturbations are due to a single crossing of the $B^2\Sigma^+$ and $C^2\Sigma^+$ states of Ne-He⁺.

An analytic function for the adiabatic curve was carefully constructed using the *ab initio* calculated points of Sidis³ as shown in Fig. 3; the small value which he obtained for the interaction term [$V_{12}(R_c) = 0.26$ eV] necessitated a sharp "knee" in the adiabatic potential. The functions $Z(l)$, $\Gamma_1(l)$, and $\Gamma_2(l)$ were found by numerical integration of set (1), and the partial-wave sum utilizing Eqs. (2) was carried to 1600 terms to evaluate the cross section.

The result showed that the predicted perturbation was located at too small an angle (about a 7° shift to the left relative to the experimental data). Putting aside uniqueness considerations, the crossing point was shifted up by 1.3 eV, as shown by the solid lines in Fig. 3. Using the new adiabatic curve, where a_0 is the Bohr radius,

$$V_a(R[a_0])[eV] = \begin{cases} e^{-5.3145R+8.6920} - e^{34.9745R-63.6537} + 18.95 & \text{for } R < 1.86a_0 \\ e^{-5.3145R+8.6920} - e^{34.9745R-63.6537} \\ + 17.50 + 1.45\exp[(R-1.86)^2/0.0841] & \text{for } 1.86a_0 < R < 1.89a_0 \\ e^{-2.074R+6.7450} + 1.45\exp[(R-1.86)^2/0.0841] & \text{for } R > 1.89a_0 \end{cases}$$

and the parameters

$$\left. \frac{dV_1}{dR} \right|_{R_c} - \left. \frac{dV_2}{dR} \right|_{R_c} = 35.0 \text{ eV}/a_0,$$

$$V_{12}(R_c) = 0.26 \text{ eV},$$

$$R_c = 1.86a_0, \quad F(R_c, l_c) = 35.74 \text{ eV}/a_0,$$

the calculation was again performed, with the result shown in Fig. 4. The perturbations in the theoretical prediction are seen to be in quantitative agreement with those resolved in the experiment. Furthermore, the qualitative aspects of the experimental cross section (a smooth decrease before and fairly smooth, with minor oscillations, after the crossing perturbation) are satisfactorily reflected by the calculation. The major difference between the relative differential cross section $c\sigma_{\text{expt}}(\theta)$ and $\sigma_{\text{calc}}(\theta)$ is in the general decay rate of the cross section.

In determining $c\sigma_{\text{expt}}(\theta)$ from the observed laboratory scattering intensity, the latter was first corrected for thermal and kinematic effects which have been discussed by Lorents and Conklin.⁵ This was done by measuring (at 5-deg intervals) the energy distribution function for the elastic channel and fitting the observed Δ_{FWHM} to a form

$$\Delta_{\text{FWHM}}(\theta) = 1 + a\theta$$

(where Δ_{FWHM} means the full width at half-maximum) and the laboratory intensities were corrected accordingly. Subsequently the normal "scattering-volume" correction was made and the appropriate Jacobian employed to retrieve $c\sigma_{\text{expt}}(\theta)$.

If one chose to equate the two functions $c\sigma_{\text{expt}}(\theta)$ and $\sigma_{\text{calc}}(\theta)$ at an angle $20^\circ < \theta < 30^\circ$, then a rather noticeable disagreement in the two functions would be observed for large scattering angles. Assuming that a normalization of $c\sigma_{\text{expt}}(\theta)$ at $\theta = 25^\circ$ to $\sigma_{\text{calc}}(25^\circ)$ is reasonable, one might ask: What *systematic* experimental error (as a function of θ) could occur for $\theta > 25^\circ$? The horizontal lines in Fig. 4 indicate a conservative estimate [$\pm 0.4\sigma_{\text{expt}}(75^\circ)$] of such a systematic error. Based on this normalization scheme, it is clear that there exists a significant difference in $\sigma_{\text{calc}}(\theta)$ and $\sigma_{\text{expt}}(\theta)$ for post-perturbation angles. Two possible explanations for this disagreement are readily apparent: (i) The *ab initio* diabatic potential [$V_1(R)$] utilized in the calculation is too "hard" for $R < R_c$; or (ii)

the two-state approximation is not sufficient; i. e., the elastic channel may be depleted for $\theta > 50^\circ$ by other nearby crossings. Specifically, the BC' crossing at $R = 1.77a_0$ (for which the final states are Ne^+ and He) perhaps plays a significant role in the collision dynamics at this collision energy. Since no measurements of the inelastic differential cross sections were made, no attempt to distinguish between these two possibilities have been made.

IV. SEMICLASSICAL INTERPRETATION

In order to discuss the origin of the observed scattering features in semiclassical terms, two pseudo-deflection-functions $\Theta_1(l)$ and $\Theta_2(l)$ have been defined:

$$\Theta_1(l) = 2 \frac{d}{dl} [\eta_a(l) + \Gamma_1(l)],$$

$$\Theta_2(l) = 2 \frac{d}{dl} [\eta_a(l) - \Gamma_2(l)].$$

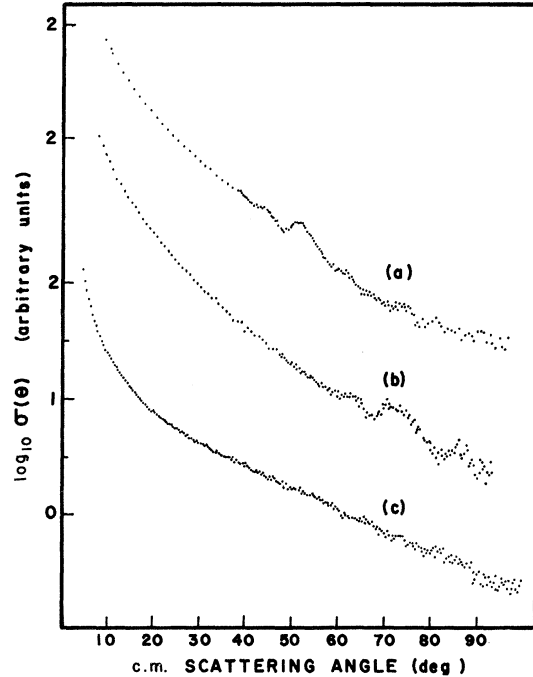


FIG. 2. Experimental differential elastic-scattering cross sections for $\text{He}^+ + \text{Ne}$ at c.m. collision energies of (a) 40 eV, (b) 30 eV, (c) 6 eV.

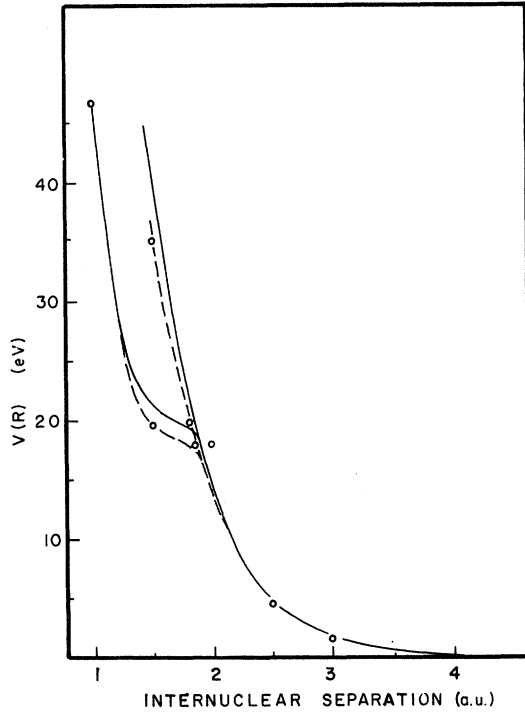


FIG. 3. Circles—result of the Sidis calculation; solid lines—analytic functions representing the adiabatic and diabatic curves corresponding to these circles; dashed line—curves which were used to calculate the differential cross section in Fig. 4.

These functions have been constructed by extending the equivalence relation to the arguments which appear in the partial-wave sum in Eq. (2).

$\Theta_1(l)$ and $\Theta_2(l)$ have been plotted along with the adiabatic and diabatic deflection functions $\Theta_a(l)$ and $\Theta_d(l)$ in Fig. 5. $\Gamma_1(l)$ is essentially a step function

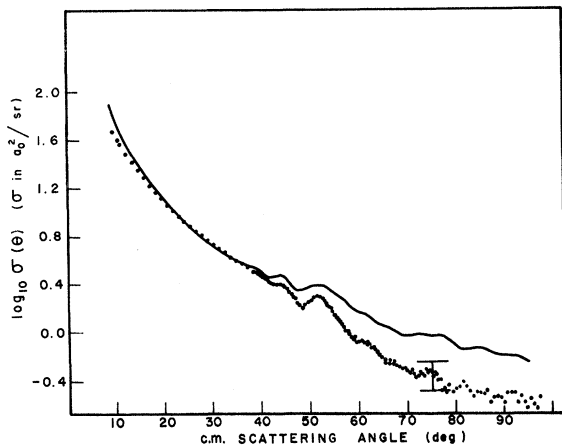


FIG. 4. Differential elastic-scattering cross section, 40-eV He⁺+Ne: solid line—calculation; points—experiment.

around l_c (the angular momentum for which the classical turning point equals R_c); this produces a negative pulse in the deflection function [$\Theta_1(l)$] which serves to decrease $\Theta_a(l)$ only in the region immediately to the left of l_c . As previously mentioned, when l becomes small

$$\Gamma_2(l) \rightarrow \eta_a(l) - \eta_d(l) - \pi,$$

so that to the left of l_c

$$\Theta_2(l) \rightarrow \Theta_d(l).$$

The difference between $\Theta_2(l)$ and $\Theta_d(l)$ is the approximately wedged-shaped region of area 2π which has been removed from $\Theta_d(l)$ around l_c .

In our numerical procedures we have not solved set (1) over the entire range of l . For $l - l_c > 16$, $Z(l)$ is almost zero and $Z^2(l)$ is entirely negligible. Consequently, for large l , the adiabatic phase shifts are all that need be calculated. Similarly, for l in the region $l_c - l > 20$, $\Theta_2(l)$ has converged to $\Theta_d(l)$. In this same region $\Gamma_1(l)$ has been extrapolated; this makes negligible difference in the resulting calculation since $\Gamma_1(l)$ has attained its limit (approximately $\frac{1}{4}\pi$) and makes no further contribution to $\Theta_1(l)$. In this region the Landau-Zener approximation has been used for $Z^2(l)$; that is,

$$Z^2(l) =$$

$$\exp \left\{ -2\pi\hbar^2 \left[\left(\frac{dV_1}{dR} \Big|_{R_c} - \frac{dV_2}{dR} \Big|_{R_c} \right) v(R_c, l) \right]^{-1} [V_{12}^2(R_c)] \right\},$$

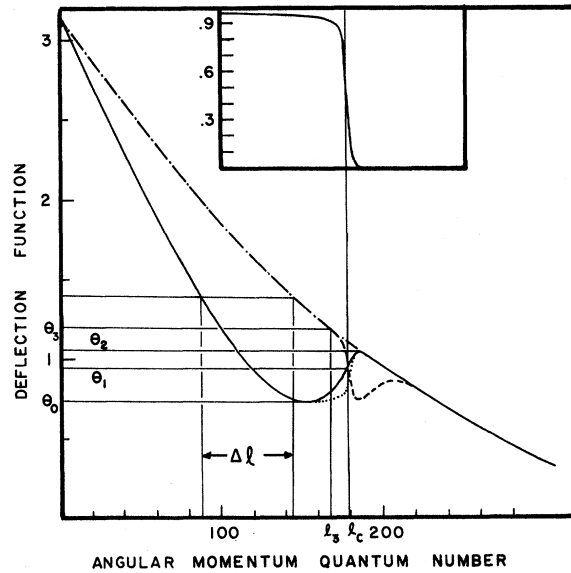


FIG. 5. Inset—the function $Z^2(l)$; solid line—adiabatic deflection function Θ_a ; chain line—diabatic deflection function Θ_d ; dashed line—the pseudo-deflection-function Θ_2 ; dotted line—the pseudo-deflection-function Θ_1 .

where $v(R_c, l)$ is the radial velocity at the crossing.

The semiclassical predictions of $\Theta_1(l)$ and $\Theta_2(l)$ for the differential cross section may now be stated; here references to angles and values of l will be to Fig. 5. For $\theta > \theta_3$ there are two paths the system may follow; i. e., $\Theta_1(l) = \Theta_a(l)$ and $\Theta_2(l) = \Theta_b(l)$. Since $Z(l)$ is almost unity, $\Theta_a(l)$ basically accounts for the differential cross section in this region. Since $Z(l)$ is not identically unity, however, there should be some small amplitude oscillations in $\sigma(\theta)$ for $\theta > \theta_3$. A straightforward semiclassical treatment, as suggested by Marchi,⁶ shows that the cross section should oscillate with periodicity

$$\Delta\theta = \frac{2\pi}{\Delta l} \quad (3)$$

and amplitude of approximately one-tenth the average intensity. Furthermore, Eq. (3) is found to be valid for all angles larger than θ_0 ; i. e., Eq. (3) predicts the periodicities of the high-frequency oscillations of the calculated differential cross sections in this angular region. Since only one classical trajectory $\Theta_1(l) = \Theta_a(l)$ exists for $\theta < \theta_0$ all oscillations are damped out in this region.

Olson and Smith^{1(e)} have pointed out that the minimum in $\Theta_a(l)$ could give rise to a rainbow-scattering effect in the differential cross section. However, by referring to the graph of $Z^2(l)$ in Fig. 5, it is apparent that the probability that the system will undergo a deflection of θ_0 is very small. Consequently, it is our belief that, while the left-most member of $\Theta_1(l)$ does contribute to the strongly damped oscillations for $\theta < 45^\circ$, the large rainbow-like envelope (at 52°) is essentially due to the negatively curved double-valued portion of $\Theta_1(l)$ immediately to the right of l_c . Since, in analogy to rainbow scattering, both this part of $\Theta_1(l)$ and the upward-opening portion of the same curve to the left of l_c would project the principal maximum of the cross section to about the same scattering angle, and since a semiclassical description is least appropriate for $l \sim l_c$ [due to the rapidly changing nature of the functions $Z(l)$ and $\Theta_{1,2}(l)$ in this region], the source of the 52° structure should be identified in a nonsemiclassical way. In order to accomplish this a large negative pulse was added to $\Theta_1(l)$ in the vicinity of its minimum by adding to the phase-shift function the additional term $3.2 \tan^{-1}[8.0/(l - 162.0)]$ and the cross section recalculated using the partial-wave sum. The results of these changes are shown in Fig. 6. Since the rainbow structure has only moved about 2° (the small amount by which the maximum of $\Theta_1(l)$ has changed is in contrast to the large change effected at its minimum), the identification of the source of the structure is believed to be correct.

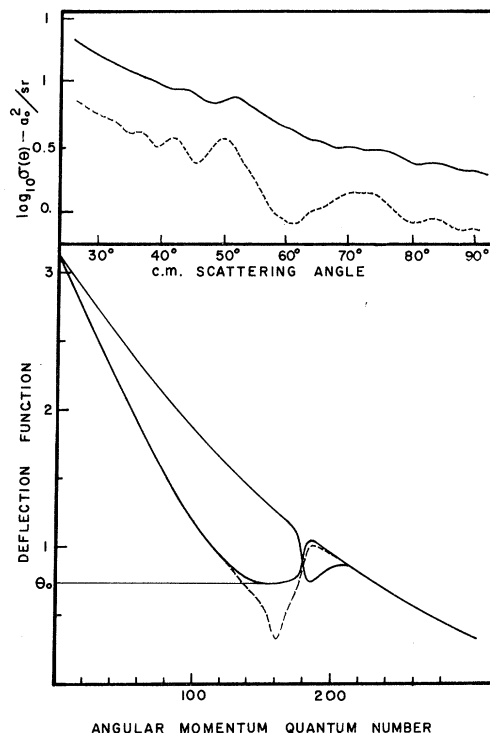


FIG. 6. (Bottom) solid lines— $\Theta_1(l)$ and $\Theta_2(l)$ from Fig. 5; dashed line—the distortion introduced into Θ_1 ; (top) solid line—convoluted differential cross section corresponding to undistorted Θ_1 and Θ_2 ; dashed line—convoluted differential cross section where Θ_1 has been distorted. Both cross sections have been calculated for the 40-eV $\text{He}^+ + \text{Ne}$ elastic-scattering system.

Also since the multiplicity of (the distorted) $\Theta_1(l)$ has been extended to include angles less than θ_0 , the higher-frequency oscillations appear at smaller angles.

V. CONCLUSION

Intermolecular potentials very similar to the *ab initio* potentials of Sidis along with the semiclassical method of Delos and Thorson have been utilized in a calculation of the elastic differential cross section and compared to the experimental results. In this particular problem ($\text{He}^+ + \text{Ne}$) the region in which the "trajectory equations" must be solved to obtain the transition probability and the corresponding phase shifts extends over a small range of angular momenta, so that the numerical work is not too formidable and the correct evaluation of these quantities is seen to provide better agreement with experiment (particularly in the elastic scattering in the region most sensitive to the crossing) than did earlier treatments of this problem. Furthermore, the

Delos-Thorson treatment lends itself to a semiclassical interpretation, which is shown to be capable of shedding considerable light on the basic physics associated with the two-state crossing problem.

ACKNOWLEDGMENTS

We would like to thank J. Delos for many valuable discussions related to his work and W. G. Rich for his assistance in obtaining the experimental data.

[†]Work supported in part by the National Science Foundation and by NASA under Grant No. NGL-47-006-055.

*Present address: Department of Chemistry, Brown University, Providence, R. I. 02912.

¹See, for example, (a) F. T. Smith, R. P. Marchi, W. Aberth, and D. C. Lorents, *Phys. Rev.* **161**, 31 (1967). (b) D. Coffey, Jr., D. C. Lorents, and F. T. Smith, *Phys. Rev.* **187**, 201 (1969). (c) F. T. Smith, H. H. Fleischmann, and R. A. Young, *Phys. Rev. A* **2**, 379 (1970). (d) R. L. Champion and L. D. Doverspike, *J. Phys. B* **2**, 1353 (1969). (e) J. Baudon, M. Barat, and M. Abignoli, *J. Phys. B* **1**, 1083 (1968). (f) J. Baudon, M. Barat, and M. Abignoli, *J. Phys. B* **3**, 207 (1970). (g) R. E. Olson and F. T. Smith, *Phys. Rev. A* **3**, 1607 (1971). (h) L. P. Kotova and M. Ya.

Ovchinnikova, *Zh. Eksp. Teor. Fiz.* **60**, 2026 (1971) [*Sov. Phys.-JETP* **33**, 1092 (1971)].

²J. B. Delos and W. R. Thorson, *Phys. Rev. Lett.* **28**, 647 (1971); *Phys. Rev. A* **6**, 728 (1972).

³V. Sidis and H. Lefebvre-Brion, *J. Phys. B* **4**, 1040 (1971); and V. Sidis, Ph. D. dissertation (University of Paris, 1971) (unpublished). The numerical values for the various potentials are only contained in the latter document.

⁴R. L. Champion, L. D. Doverspike, W. G. Rich, and S. M. Bobbio, *Phys. Rev. A* **2**, 2327 (1970).

⁵D. C. Lorents and G. M. Conklin, *J. Phys. B* **5**, 950 (1972).

⁶R. P. Marchi, *Phys. Rev.* **183**, 185 (1969).

Ionization of He($1s^2$) and Li⁺($1s^2$) by Hydrogen-Atom Impact

M. R. Flannery

School of Physics, Georgia Institute of Technology, Atlanta, Georgia 30332

(Received 7 August 1972)

A semiquantal theory based on a binary-encounter approach is applied to the examination of the ionization of He($1s^2$) and Li⁺($1s^2$) by the impact of hydrogen atoms in their ground state with incident energy E above 10 keV. Simultaneous excitations of the projectile atom are explicitly acknowledged. The use of Born's approximation for electron-atom elastic and inelastic-scattering results in satisfactory agreement with the Born cross sections for atom-atom collisions.

I. INTRODUCTION

Theoretical descriptions of inelastic collisions at intermediate and high impact energies between two neutral atoms have been limited to the application of the Born approximation for ionization¹⁻³ and at most to multistate impact-parameter treatments for excitation.⁴⁻⁶ A Born calculation of a hydrogen-hydrogen ionization collision requires the evaluation of a four-dimensional integral, and for cases involving more complex systems, computations of even the Born approximation would be lengthy unless extremely simple electronic wave functions were employed. The introduction of refinement to these calculations on ionization would prove so prohibitively difficult in practice that other approaches to the ionization problem must be sought. Moreover, the laboratory production of more intense neutral atomic beams, and the more accurate detection of low-intensity neutral beams have now made the experimental study of neutral-neutral collisions more feasible, and theoretical data on complex atomic systems are somewhat scant.

In an effort to treat complex systems, Flannery⁷ has recently developed a semiquantal model that is based on the binary-encounter approach for inelastic collisions involving heavy neutral particles. The incident projectile atom is assumed to collide with each electron, considered to be singly active and bound to a passive core, in such a way that the internal energy of the electron-core system is either increased for excitation or decreased for deexcitation. Ionization occurs when the electron becomes detached from the target atom. The possibility that excitation, deexcitation, or ionization arises in the projectile can also be theoretically acknowledged. Details of the active electron-neutral projectile interaction are furnished by the use of the corresponding elastic or inelastic differential (quantal) cross sections σ_{eA} for scattering of the valence electrons by the incident atom. The core of the target atom is ignored except insofar as its interaction with the active electron generates a distribution f_{nlm} in the momentum of the electron, bound to the target atom in quantum state (nlm). Also, for the nonhydrogenic target systems to be treated here, allowance is made for the shadow